A Turmitobionic Method for the Solution of Magnetic Defectometry Problems in Structural–Parametric Optimization Formulation

V. Ya. Galchenko* and A. N. Yakimov**

Lugansk State Medical University, kvartal Pyatidesyatiletiya Oborony Luganska 1, Lugansk, 91045 Ukraine
*e-mail: halchvl@gmail.com
**e-mail: alex_forever_82@mail.ru
Received June 25, 2013

Abstract—A turmitobionic method based on the structural–parametric optimization formulation of a problem has been proposed for the solution of the inverse problem of magnetic nondestructive testing. A solution is found with consideration for the finite dimensions of flaws and a test object and the nonlinearity of the magnetic characteristics of a ferromagnet.

INTRODUCTION

In recent years, the main efforts of researchers during magnetic nondestructive testing (NDT) have been focused on the problems of evaluating the shape and geometric dimensions of detected continuity flaws. The division of the methods that are oriented to the solution of similar problems into the phenomenological and algorithmic classes in the terms proposed in [1] is well known. The advantages and disadvantages of each class were also repeatedly noted in [2–4], and, although there is no consensus of opinion as to the prospects of the use of a particular class, the analysis of the works in this field shows a definite preference of researchers for the first of them. This is indicated by the works of both Russian and foreign scientists [5, 6, 7–11], in which the methods of this class are mentioned as flaw-shape reconstruction methods.

The problem of the reconstruction of a flaw from the magnetic field intensities measured in a test zone may be considered as a particular case of the more general problem of the synthesis of magnetic field sources with ferromagnetic structural elements and a specified field distribution in the working zone [12, 13]. Assuming that the magnetic intensities measured in a test zone represent an a priory specified field configuration in the working zone of a source, the problem is formulated as the search for the shape of a ferromagnet (a test object with a flaw) for specified primary sources (a system for the magnetization of a test object), i.e., the inverse problem is solved.

The problem of the reconstruction of a flaw from the fields measured in a test zone in optimization formulation is characterized by the number of mathematical peculiarities that complicate its solution. The universality of the solution approach to the inverse problem, which implies considerable arbitrariness in the considered shapes of continuity flaws, can be provided only with numerical methods. Since the direct field-calculation problem is solved several times in this case, a necessary condition for its software implementation is an efficient numerical algorithm (from the viewpoint of time expenditures and computational resources). It should also be taken into consideration that the solved problems have a three-dimensional character, which enables the consideration of finite-size flaws on test objects of arbitrary shapes and limited sizes. The nonlinear characteristics of a ferromagnetic material in close-to-saturation magnetization fields should also be taken into account.

The incorrect formulation of the optimizingly solved inverse problem is manifested as the multidimensional "ravine" topography of a target function, thus requiring special mathematical approaches to its solution. Moreover, a found solution must be a global extremum. It should also be taken into account that the target function is specified algorithmically as a result of the numerical solution of the magnetic-field
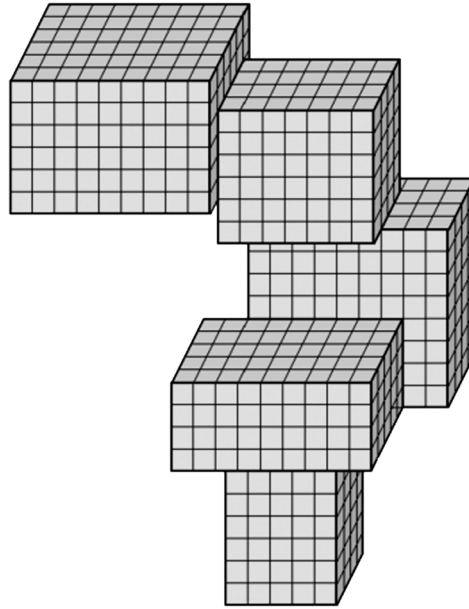
Fig. 1. An example of a structure formed by a set of five primitives.

analysis problem. Due to cumbersome calculations, rigid requirements are imposed on an optimization algorithm as to the number of target-function iterations that provide convergence to a global optimum, even when the direct problem must be solved only once.

In [1−11], all these requirements were not met simultaneously, although the authors of [5, 6] came closest to the fulfillment of the entire set of requirements. However, the software proposed in these works is not oriented to solving direct problems of high dimensions, as is typical for NDT and proven by the numerical experiments performed in [14−17], where the discretization step that was used to obtain correct results was several fractions of a millimeter. In these works, the authors restricted their consideration to the search for a local target-function optimum and confined the solution of the problems to parametric synthesis, thus enabling the use of redundantly or insufficiently complicated ferromagnet structures. The redundancy of a structure unreasonably increases the dimension of a problem and its insufficiency prevents solution in principle. The optimal selection of the number of structural elements is possible only for the structural−parametrical formulation of the synthesis problem [18]. The same issue makes topological optimization [19] unsuitable for use, as was rightly noted in [5].

The objective of this paper is to develop a method for the solution of inverse NDT problems in the structural−parametric optimization formulation with consideration for the entire set of the above-listed requirements.

PROBLEM FORMULATION

Let us briefly state the idea of this approach to the solution of inverse problems for the testing of an object by the superposed field method, which is highly efficient with respect to soft-magnetic products of rather complicated geometries. A test object may have surface or subsurface continuity flaws of arbitrary shapes and finite sizes. The material of a test object is considered to be isotropic and non-linear and hysteresis phenomena are not taken into account. The test object is magnetized with constant magnetic fields, $\vec{H}_0$. The leakage fields produced by a flaw are measured in the general case in a space, which is called the test zone here and below, which is located near the surface of a test object and has a finite size. It is necessary to determine the shape of a test object with consideration for a continuity flaw cavity in it, i.e., to reconstruct the shape of a test object with existing flaws, from the magnetic field intensities measured in a test zone.
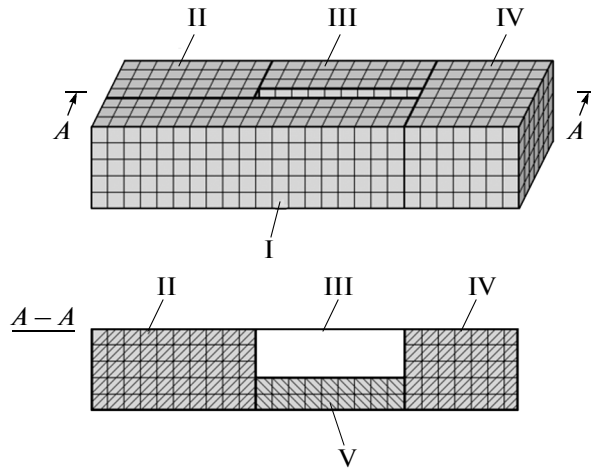
Fig. 2. A test object formed by a set of five primitives with a surface flaw in the form of a crack.

For further reasoning, let us discretize a flaw-free test object and a certain area, which belongs to the space surrounding it and incorporates the test zone, with the use of a regular spatial grid consisting of rectangular prismatic microelements.

Let us introduce the concept of the structure of a test object. The structure of a test object is a set of primitives, which are understood to mean elementary geometric objects that are can reasonably be divided into smaller parts. In this study, it is convenient to represent primitives as rectangular prisms, whose geometric dimensions can be determined at an accuracy of up to a partitioning grid microelement. The set of primitives, each of which is adjacent at least to a single primitive from the entire set, forms the structure of a test object (Fig. 1). The five-primitive structure of a test object with a surface rectangular continuity flaw in the form of a crack is shown in Fig. 2. The search for a structural variant that provides the measured field distribution in the test zone was the key problem of this study. In other words, it is necessary to determine the number of primitives and their geometric dimensions, which will eventually constitute an inverse problem solution facilitated by the fact that the initial geometry of a flaw-free test object is known a priory, and the problem is simplified to the search for the structure of a flaw cavity.

SOLUTION OF THE DIRECT PROBLEM

The mathematical model of the direct problem, which consists in evaluating the magnetic-field distribution in a test zone for a test object of known geometry, is based on the non-linear integral equation

$$\vec{H}(Q) = -\frac{1}{4\pi}\text{grad}_Q \iiint_V \vec{M}(P)\text{grad}_P \frac{1}{r_{PQ}} dV_P + \vec{H}_0(Q) \tag{1}$$

complemented with the non-linear material equation

$$\vec{M} = F(\vec{H}), \tag{2}$$

where P is a point that belongs to the area V occupied by a ferromagnet, Q is an observation point, $\vec{r}_{PQ} = \vec{r}_Q - \vec{r}_P$ is the vector directed from point P to point Q, $\vec{H}$ is the magnetic field intensity, $\vec{M}$ is the magnetization of a ferromagnet, and F is the non-linear operator of the magnetic characteristic of a material.

For N partitionings of a test object, this equation can be written as

$$\vec{H}(Q) = -\frac{1}{4\pi}\text{grad}_Q \sum_{j=1}^{N} \iint_{V_j} \vec{M}(P)\text{div}_P\left(\frac{1}{r_{PQ}}\right) dV_P + \vec{H}_0(Q). \tag{3}$$

Assuming the uniform magnetization of each spatial grid element filled with a ferromagnetic material, we reduce Eq. (3) to the form

$$\vec{H}_t = -\frac{1}{4\pi}\text{grad}_Q\sum_{j=1}^{N}\iiint_{V_j}\text{div}_P\left(\frac{\vec{M}(P)}{r_{PQ}}\right)dV_P + \vec{H}_0(Q), \tag{4}$$

which in turn can be transformed for the field intensity $\vec{H}_i$ ($i = \overline{1, N}$) in the center of the ith elementary volume by passing from the integration over the volume to the integration over the surface with consideration for the fact that $\vec{M}_j$ is the magnetization of the jth elementary volume into the equation

$$\vec{H}_i = -\frac{1}{4\pi}\text{grad}_Q\sum_{j=1}^{N}\oint_{\partial V_j}\int\frac{\vec{M}_j}{r_{PQ}}d\vec{S}_P + \vec{H}_{0i}(Q), \tag{5}$$

where $\vec{H}_{0i}$ is the corresponding magnetizing field intensity, and ∂V is the surface area of each elementary volume. Changing the order of the integration and gradient calculation operations, we write Eq. (5) as

$$\vec{H}_i = \frac{1}{4\pi}\sum_{j=1}^{N}\oint_{\partial V_j}\int\frac{(\vec{M}_j \cdot \vec{n}_P)\vec{r}_{PQ_j}}{r_{PQ_j}^3}dS_P + \vec{H}_{i0}(Q), \ \ i = \overline{1, N} \tag{6}$$

The mathematical model for solving the direct problem is written in the matrix form as the equation system

$$\begin{cases} \mathbf{H} = \mathbf{A} \cdot \mathbf{M} + \mathbf{H}_0, \\ \mathbf{M} = \mathbf{F(H)}, \end{cases} \tag{7}$$

where $\mathbf{A}$ is an elemental volume influence matrix consisting of 3×3 matrix blocks, $\mathbf{A}_{ij}$, which take into account the contribution of the magnetization of the jth elementary volume to the field intensity in the ith elementary volume, $\mathbf{H}$ is the column vector of the magnetic field intensity in microelement volumes, $\mathbf{H}_0$ is the column vector of the magnetizing field intensity in the gravity centers of discretization microelements, $\mathbf{M}$ is the column vector of the magnetization in discretization microelements, and

$$\mathbf{F(H)} = \begin{pmatrix} \vec{M}_1 \\ \vec{M}_2 \\ \dots \\ \vec{M}_N \end{pmatrix} = \begin{pmatrix} F_1(\vec{H}_1) \\ F_2(\vec{H}_2) \\ \dots \\ F_N(\vec{H}_N) \end{pmatrix}, \tag{8}$$

where $\vec{M}_j = F_j(\vec{H}_j)$ is the magnetic characteristic of the jth elementary volume. Note that the elements of matrix blocks $\mathbf{A}_{ij}$ are determined via the integration over six rectangles that constitute the surface of a discretization microelement by analogy with [20], where this procedure was described in detail.

The discretization microelement magnetizations $\vec{M}_j$ are found from Eqs. (7) using the non-linear magnetic characteristic approximation similar to [14−16] and the parameter continuation method in compliance with the technology described in [16]. Using the found distribution of magnetizations, the information magnetic-field intensity $\vec{H}(Q)$ at an arbitrary observation point Q, which is situated in the test zone and does not belong to any elementary volume boundary, is calculated as

$$\vec{H}(Q) = \frac{1}{4\pi}\sum_{j=1}^{N}\oint_{\partial V_j}\int\frac{(\vec{M}_j \cdot \vec{n}_P)\vec{r}_{PQ}}{r_{PQ}^3}dS_P + \vec{H}_0(Q). \tag{9}$$

In the numerical solution of a system of non-linear high-order equations typical for NDT problems by the Newton−GMRES method, the construction of a Krylov subspace is the most resource-consuming
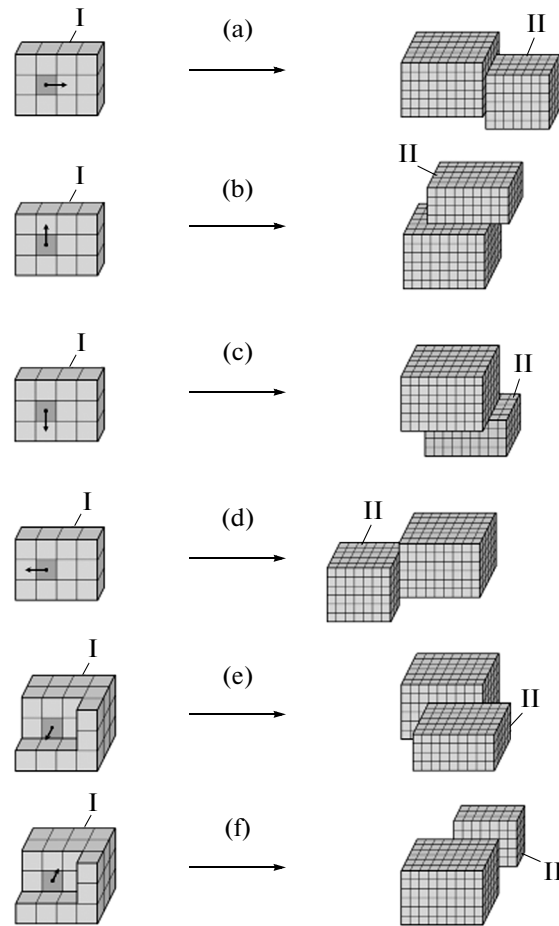
Fig. 3. Building up of a structure via the sequential addition of primitives: I is the life area of a turmite, II is the domain of the formation of the spatial geometry of a structure.

stage due to the iteratively repeated multiplication of a Jacobian matrix by a column residual vector [21]. The acceleration of this operation, which is especially appreciable with an increase in the system dimension, is feasible with a number of algebraic transformations, e.g., the conversion of a linear convolution into a circular convolution and the subsequent application of direct and inverse fast Fourier transforms similar to those shown in [21]. However, this imposes additional requirements on the generation of a spatial-discretization grid, where the number of microelements must be selected as equal to a certain power of two. As a result of such manipulations, the time of matrix–vector operations is reduced by several orders of magnitude. Moreover, a high speed of calculations in the case of its implementation is provided by the parallelization of processes on NVIDIA graphic processors with the CUDA technology.

INVERSE PROBLEM SOLUTION

The method of solving the inverse problem in structural-parametric optimization formulation implies the determination of an optimal flaw-containing test-object structure formed by a minimum number of primitives. Hence, optimization has to be performed over the multi-criteria target function

$$f(\mathbf{X}) = \varphi_1(H) + \varphi_2(L_{\mathrm{pr}}) \to \min, \tag{10}$$

where $\mathbf{X}$ is the vector of varied parameters, $\varphi_1(H)$ is the target function component specifying the requirements to the magnetic field distribution in a test zone, $\varphi_2(L_{\mathrm{pr}})$ is the component specifying the number of structure-forming primitives, and L_{pr} is the number of primitives.

The vector of varied parameters has a variable length at each optimization cycle iteration depending on an analyzed test object structure variant. The first component of the target function is determined algo-
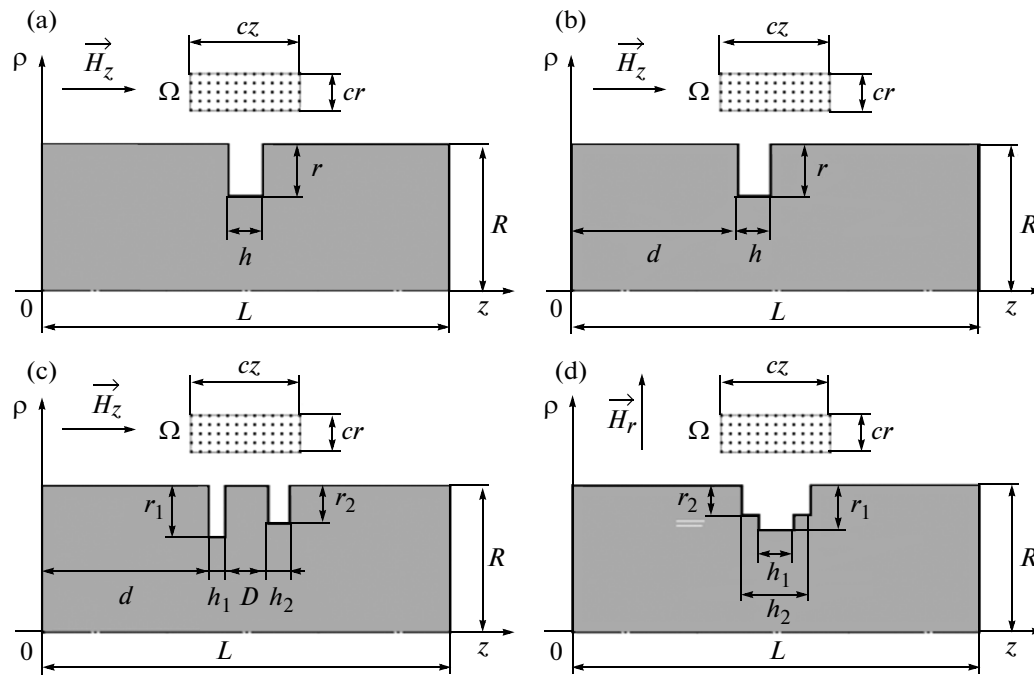
Fig. 4. The types of considered flaws and their parameters: (a) a single flaw with a test zone placed symmetrically above it, (b) a single flaw with a displaced test zone, (c) a group of two flaws, (d) flaws with complex shapes.

rithmically and represents the normalized residual between the field intensities, which are measured in a test zone and numerically calculated at the same spatial test points for a current structural variant by solving the direct problem. The technique of searching for the global optimum of the target function in multi-criteria formulation is identical to the method described in [21, 22] and based on the algorithm of global multi-agent bionic particle swarm optimization (PSO) with the evolutionary formation of a swarm composition [13, 23]. A peculiarity of this algorithm is a high convergence rate and the orientation to search for the solutions of algorithmically specified multidimensional "ravine" target functions. The algorithm uses the evolutionary strategy for the organization of the topology of links between swarm particles in its operation and applies the genetic operators of crossover and mutation to swarm particles, subjecting not only the coordinates of swarm particles, but also their velocities and the links between them to crossover.

The outer loop of the structural-parametric synthesis procedure is designed for the selection of an optimal test-object structure. Test-object structures that are considered as possible candidates are generated using binary turmites, a kind of cellular automation, that via three-dimensional Turing machines [24]. In contrast to a two-dimensional Turing machine, a turmite can move in space over a cellular grid and not merely left, right, and forward as in the classic case. When test-object structures are generated, two conditional domains, such as the domain that represents the life area of a spatial turmite and the domain of the formation of a spatial structural geometry, are put into consideration. The cellular region of the life area of a turmite does not belong to the initially introduced grid of discretization into microelements, but has an abstract character and serves only as an auxiliary mean for the construction of a structural variant. Each step of a turmite in the cellular region of the life area is a command for the addition of a corresponding arbitrarily-sized primitive to the current structural geometry of a test object in the domain of its formation, thereby building up the structure via the addition of new elements to the initial variant (Fig. 3). The building up of a structure is targeted, as the behavior of the motion of a turmite is specified in compliance with the rules that lead to the improvement of target-function values, thus evaluating intermediate structure variants.

During the evaluation of a structural variant, the parametric synthesis procedure that provides the evaluation of the optimal geometric dimensions of structure-forming primitives with an accuracy of up to a discretization grid microelement is performed in the embedded loop of the algorithm. The "intelligence" of a turmite grows as a result of adaptation to the most promising directions of the random search for an
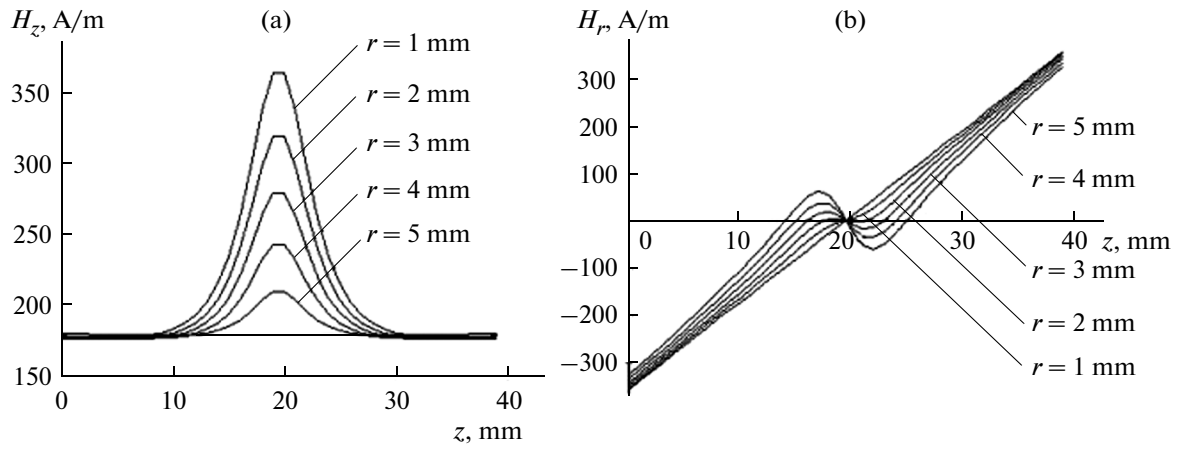
Fig. 5. The distribution of (a) the axial and (b) radial components of the magnetic-field intensity above the surface of a single flaw with a test zone placed symmetrically above it.
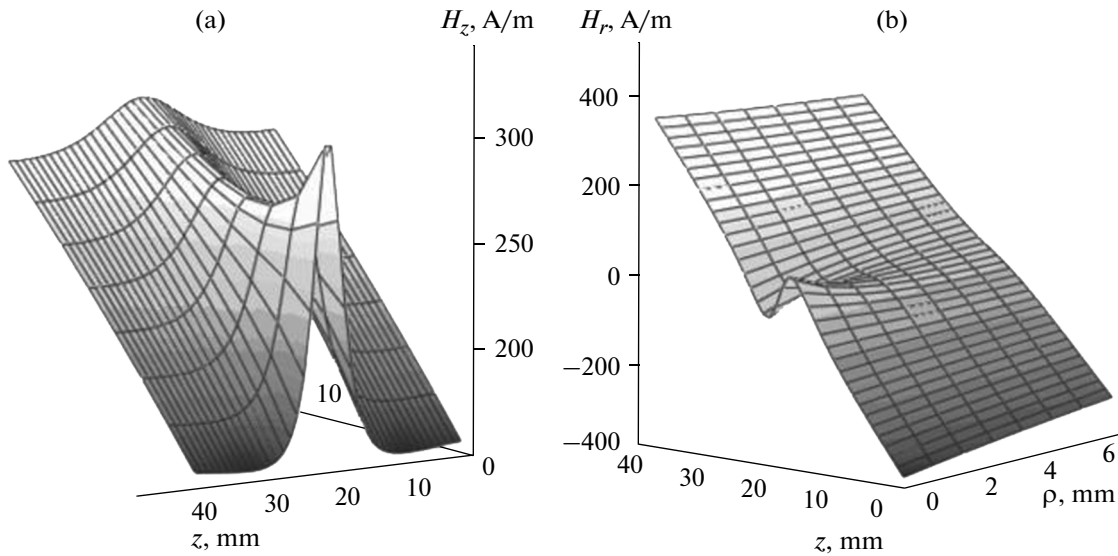

Fig. 6. The distribution of (a) the axial and (b) radial components of the magnetic-field intensity above a single flaw ($h = 1$ mm, $r = 3$ mm).
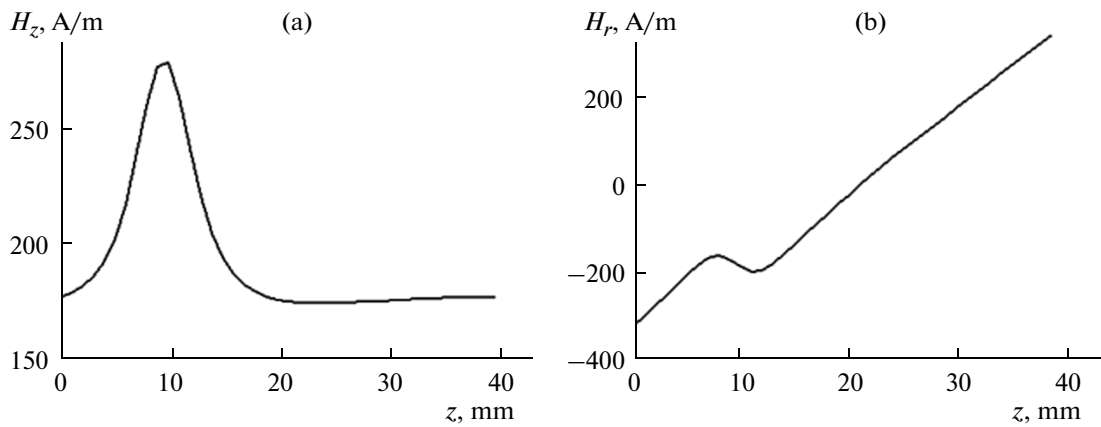

Fig. 7. The distribution of (a) the axial and (b) radial components of the magnetic-field intensity above a single flaw (see Fig. 4b): $R = 3$ mm, $h = 1$ mm, $d = 44.5$ mm.

Table 1. Results for solving the inverse problem for a single flaw (see Fig. 4a)

Flaw no.	Flaw parameters		Inverse-problem solution results		
	width h, mm	depth r, mm	number of iterations	found target-function value	ield synthesis error
1		1	5	1.4×10^{-6}	0.011
2		2	10	6.7×10^{-6}	0.033
3	0.5	3	22	1.7×10^{-5}	0.025
4		4	26	2.9×10^{-6}	0.024
5		5	34	7.0×10^{-6}	0.020
6		1	5	1.6×10^{-6}	0.015
7		2	16	2.9×10^{-6}	0.028
8	1	3	15	5.5×10^{-6}	0.042
9		4	11	7.8×10^{-7}	0.076
10		5	16	3.5×10^{-7}	0.023
11		1	11	5.8×10^{-6}	0.072
12		2	6	4.9×10^{-6}	0.037
13	2	3	4	2.3×10^{-6}	0.046
14		4	14	3.6×10^{-6}	0.083
15		5	12	8.4×10^{-4}	0.068
16		1	15	3.2×10^{-6}	0.080
17		2	5	6.9×10^{-6}	0.032
18	3	3	18	2.3×10^{-6}	0.037
19		4	20	7.5×10^{-6}	0.068
20		5	9	2.3×10^{-5}	0.041

optimum. The strategy of a search is based on the probabilistic evaluation of exploratory steps and the escape from deadlock search lines is provided via the memorization of the previous steps of the trajectory of a motion with the subsequent correction of a history vector and is governed by the memory depth as an algorithmic parameter, i.e., targeted self-training search is performed [25].

The targeted search for the structure of a test object is stopped when the requirement for the minimum deviation of the field topography measured in a test zone from the field topography created by a generated test-object structure is met.
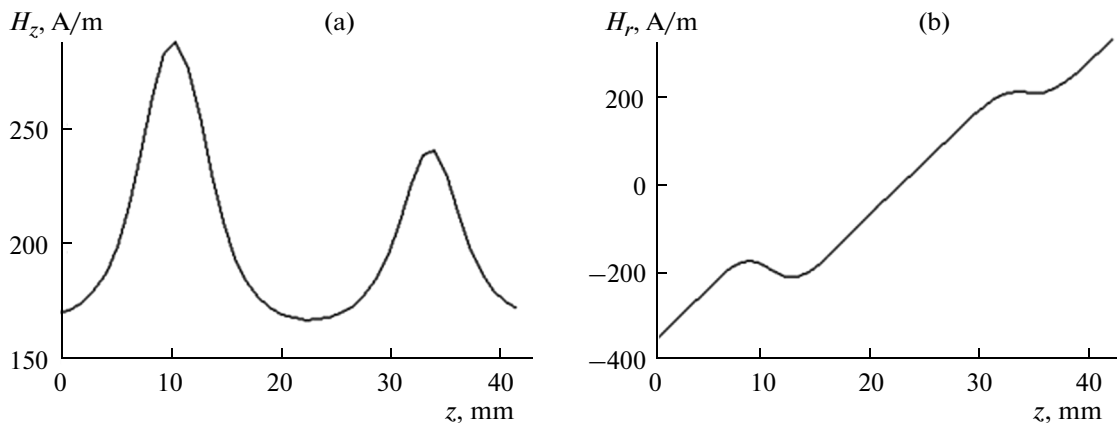

Fig. 8. The distribution of (a) the axial and (b) radial components of the magnetic-field intensity above a group of two flaws (see Fig. 4c): $h_1 = 1$ mm, $r_1 = 3$ mm, $h_2 = 1.5$ mm, $r_2 = 2$ mm, $d = 44$ mm, $D = 9.5$ mm.
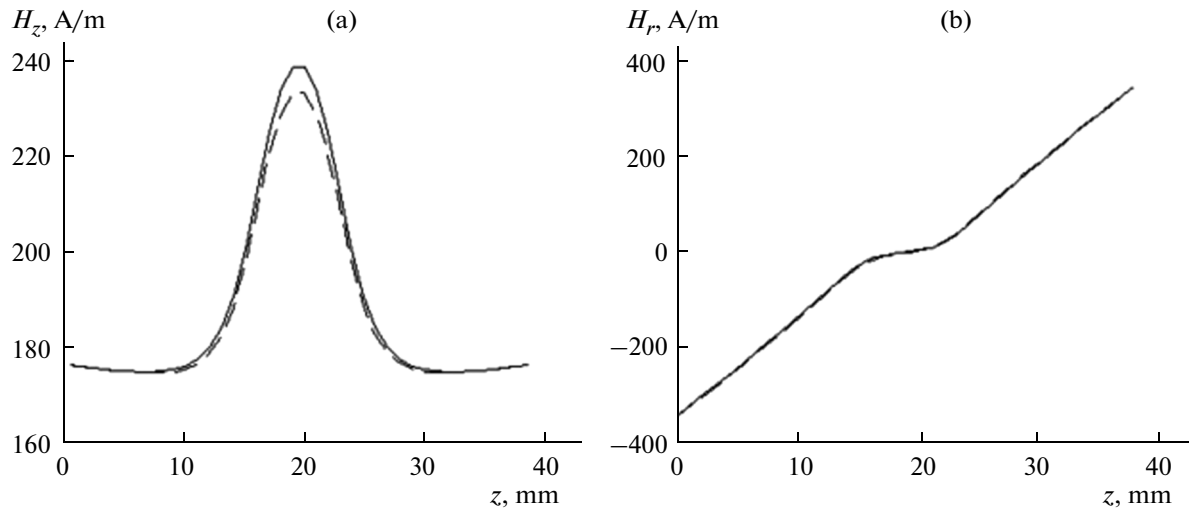
Fig. 9. The distribution of (a) the axial and (b) radial components of the magnetic-field intensity above a flaw with a complex shape (see Fig. 4d) in the case of axial magnetization: $h_1 = 1$ mm, $r_1 = 2$ mm, $h_2 = 5$ mm, $r_2 = 0.5$ mm.

VERIFICATION OF THE SOLUTION METHOD FOR THE INVERSE PROBLEM

Let us check the efficiency of the proposed approach, using software that is oriented to the solution of problems for test objects that have axial symmetry properties [13, 21, 22] and are a particular case of a more general problem. Numerical experiments were performed for the following NDT cases (Fig. 4): a single flaw with a test zone placed symmetrically above it, a group of two flaws of different sizes, and a with complex shapes flaw with a complex shape. The test object has the following parameters: the length $L = 100$ mm and the radius $R = 15$ mm.

The material from which the test object was manufactured had a nonlinear magnetic characteristic and was approximated by a dependence with the same numerical parameters as in [13−17]. For axial symmetry, the test zone was shaped like a rectangle that had the dimensions $cz = 40$ mm and $cr = 5$ mm and contained K 0.5-mm spaced test points. The gap between the test zone and the test object was 1.25 mm. The test object was magnetized by a constant magnetic field with an intensity of 1 kA/m and magnetization was performed axially in some cases and radially in other cases; however, the field intensity remained constant. All the calculated field distribution dependences are given at a fixed height of 1.75 mm above the test object. The microelement discretization grid had a step of 0.5 mm, unless otherwise specified.

In all the numerical examples, the target-function component $\varphi_1(H)$ has the following form:

$$\varphi_1(H) = \sum_{i=1}^{K} \frac{(H_{zi}^{(\text{req})} - H_{zi})^2 + (H_{ri}^{(\text{req})} - H_{ri})^2}{(H_{zi}^{(\text{req})})^2 + (H_{ri}^{(\text{req})})^2}, \tag{11}$$

where $H_{zi}^{(\text{req})}$ and $H_{ri}^{(\text{req})}$ are the axial and radial magnetic field-intensity components measured at the ith test point, and H_{zi} and H_{ri} are the same parameters determined by solving the direct problem. The dependences plotted in Figs. 5 and 6 for a single continuity flaw (see Fig. 4a) indicate the correct operation of the software and allow us to go to the solution of more complicated problems.

Table 2. Results for solving the inverse problem for a flaw with a complex shape

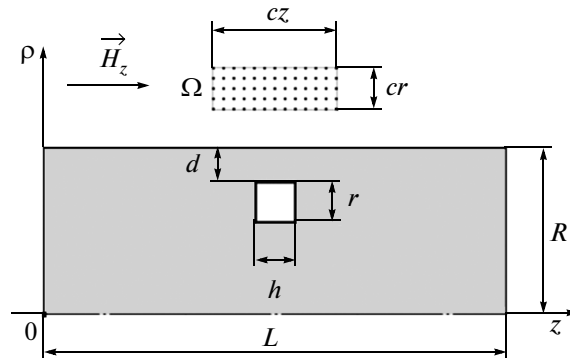| Test-zone magnetization type	Found flaw parameters				Inverse-problem solution results		
	h_1, mm	r_1, mm	h_2, mm	r_2, mm	number of iterations	found target-function value	field-synthesis error, %
Axial	4	1.5	16	0	38	335.5	3.063
Radial	1	2	5	0.5	34	4.9×10^{-6}	0.026

Fig. 10. The parameters of a single subsurface flaw: $H = 1$ mm, $r = 2$ mm, $d = 1$ mm.

The results of solving the inverse problem for this case are listed in Table 1. Note that the microelement discretization grid for flaws with a width $h = 0.5$ mm had a step of 0.25 mm. The flaw dimensions were precisely determined in all the cases in ~14 iterations on average.

The NDT case, whose geometric model is shown in Fig. 4b, is illustrated in Fig. 7; in this case, the flaw parameters were precisely determined in 33 iterations, the target function was 8.3×10^{-6}, and the relative synthesis error did not exceed 0.059%.

Let us complicate the situation and consider the NDT case for a group of two flaws (see Fig. 4c). The corresponding field-distribution dependences are plotted in Fig. 8. Note that the field distribution distinction between the flaws disappears at a parameter $D = 5-6$ mm. When the distinction exists, the dimensions of the flaws can precisely be determined in 37 iterations; the target function amounts to 1.5×10^{-5} and the relative synthesis error for the geometry of the flaws that is found does not exceed 0.101%.

The NDT case that is shown in Fig. 4d may be classified among the cases that give rise to some difficulties in solving the inverse problem. Such a test object was subjected to both axial and radial magnetization. In the first case, desirable solution results were not attained, but a flaw of a different geometry with a field distribution that was similar to the real leakage-field distribution was found (the dashed curve in Fig. 9). The study results are given in Table 2, which also contains the data for the precise evaluation of the flaw dimensions for the second type of magnetization.

The case of detecting a subsurface flaw in a test object is also of particular interest and has the geometric model shown in Fig. 10. The corresponding leakage-field distribution dependences are illustrated in Fig. 11. In
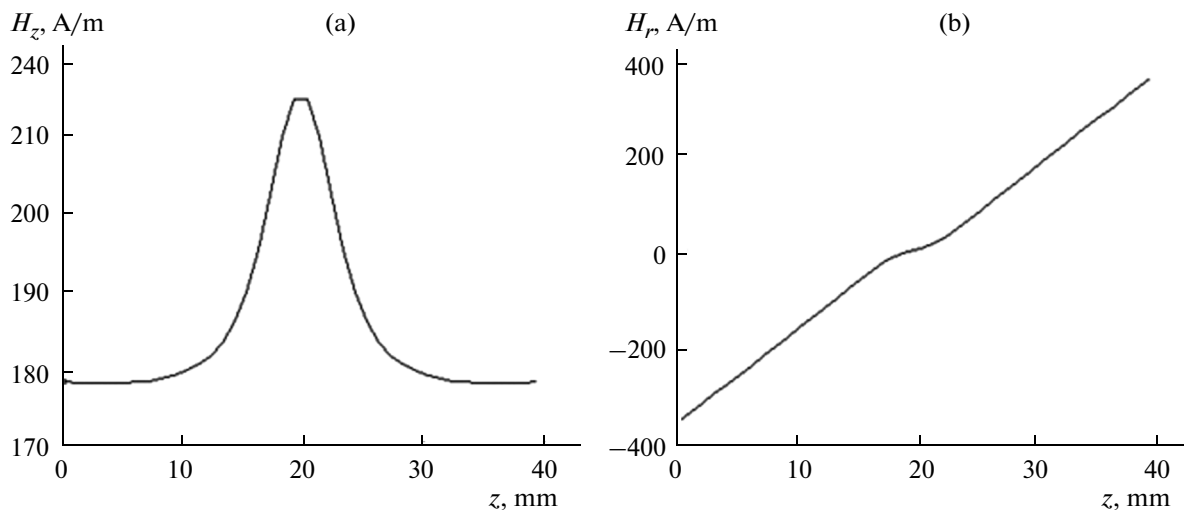

Fig. 11. The distribution of (a) the axial and (b) radial components of the magnetic-field intensity above a single subsurface flaw.
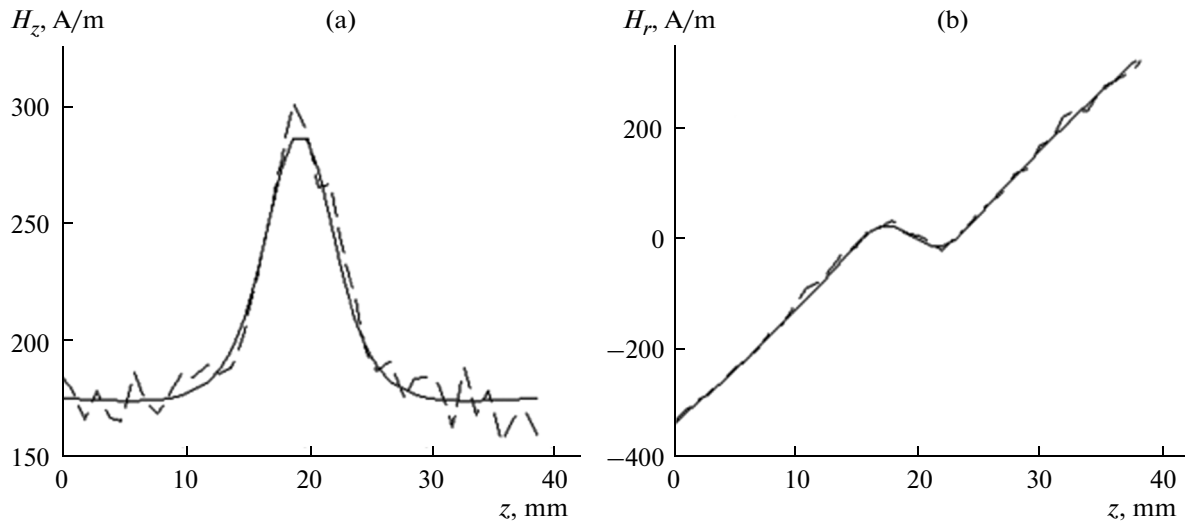
Fig. 12. The distribution of (a) the axial and (b) radial components of the magnetic-field intensity above the surface of a single flaw at a 10% noise level in a signal (see Fig. 4a) at $h = 2$ mm and $r = 3$ mm.

this case, the defectometry problem was also precisely solved in seven iteration cycles. The target function took on the value of 2.1×10^{-5}, and the relative field synthesis error did not exceed 0.043%.

When the flaw depth r was increased to 4–5 mm, some errors in the evaluation of the true value of this parameter were observed, although the flaw width, h, was determined precisely in all the cases.

In conclusion, let us consider the operation of the software in the case of noisy magnetic-field intensities measured in a test zone and evaluate the stability of the applied mathware. To accomplish this, we superimposed noise onto the signal from a flaw, thus simulating the measurement process characterized by the presence of a random component. The noise was generated in compliance with the normal distribution law within a range of $\pm 3\sigma$, where σ was the constant component of the maximum signal from a flaw (dashed curve in Fig. 12).

The results of the numerical modeling with the precise evaluation of flaw dimensions are listed in Table 3 and the target function in this case has the form

$$\varphi_1(H) = \sum_{i=1}^{K} \frac{(H_{zi}^{(noise)} - H_{zi})^2 + (H_{ri}^{(noise)} - H_{ri})^2}{(H_{zi}^{(noise)})^2 + (H_{ri}^{(noise)})^2}, \tag{12}$$

where $H_i^{(noise)}$ is the noisy measured intensities of the magnetic-leakage field of a flaw in a test zone. Note that the solution of the inverse problem turned out to be practically impossible at a noise level above 30%.

Table 3. The results of solving the inverse problem for a single flaw and a noisy signal measured in a test zone

Noise level, %	Found flaw parameters		Inverse-problem solution results		
	h, mm	r, mm	number of iterations	found target-function value	field-synthesis error
5	2	3	6	7.2×10^3	4.793
10	2	3	8	2.9×10^4	9.696
20	2	3	3	1.2×10^5	19.708
30	1.5	3	22	2.6×10^5	29.765

CONCLUSIONS

A turmitobionic method for the solution of the inverse NDT problem in structural-parametric optimization formulation with the search for a global extremum and consideration for the spatial character of a flaw leakage field and the nonlinearity of the magnetic characteristics of a material has been proposed.

The efficiency of the proposed approach has been demonstrated on model examples in the solution of inverse problems for the testing of objects with axial symmetry properties.

The solutions for both simply shaped flaws and cases that are more problematic for NDT, such as flaws with complex shapes, groups of flaws, subsurface flaws, and noisy signals of measurements in a test zone, have been obtained.

REFERENCES

1. Lunin, V.P., Phenomenological and algorithmic methods for the solution of inverse problems of electromagnetic testing, *Rus. J. Nondestr. Test.*, 2006, vol. 42, no. 6, pp. 353−362.

2. Pechenkov, A.N. and Shcherbinin, V.E., Software for solving inverse magnetostatic problem with a view to calculating flaw parameters, *Rus. J. Nondestr. Test.*, 2001, vol. 37, no. 6, pp. 422−425.

3. Han, W. and Que, P., 2D defect reconstruction from MFL signals by a genetic optimization algorithm, *Rus. J. Nondestr. Test.*, 2005, vol. 41, no. 12, pp. 809−814.

4. Krotov, L.N., Reconstruction of a media boundary based on the spatial distribution of stray magnetic fields. II. Definition and method of solving the inverse geometric problem of magnetostatics, *Rus. J. Nondestr. Test.*, 2004, vol. 40, no. 6, pp. 385−390.

5. Pechenkov, A.N., A mathematical algorithm for solving the inverse problem of magnetostatic flaw detection, *Rus. J. Nondestr. Test.,* 2005, vol. 41, no. 11, pp. 714−718.

6. Pechenkov, A.N. and Shcherbinin, V.E., On the solution of the inverse problem of magnetostatic tomography, *Rus. J. Nondestr. Test.*, 2009, vol. 45, no. 3, pp. 176−190.

7. Calvano, F., Electromagnetic non-destructive evaluation and inverse problems, *Ph.D Thesis,* Naples: Univ. Naples Federico II, 2010.

8. Han, W. and Que, P., An improved genetic local search algorithm for defect reconstruction from MFL signals, *Rus. J. Nondestr. Test.,* 2005, vol. 41, no. 12, pp. 815−821.

9. Huang, H., Takagi, T., and Ushimoto, T., Crack shape reconstruction in ferromagnetic materials using a novel fast numerical simulation method, *IEEE Trans. Magn.,* 2004, vol. 40, no. 2, pp. 1374−1377.

10. Chen, Z., Preda, G., Mihalache, O., and Miya, K., Reconstruction of crack shapes from the MFLT signals by using a rapid forward solver and an optimization approach, *IEEE Trans. Magn.,* 2002, vol. 38, no. 2, pp. 1025−1028.

11. Li, Y., Udpa, L., and Udpa, S.S., Three-dimensional defect reconstruction from eddy-current NDE signals using a genetic local search algorithm, *IEEE Trans. Magn.*, 2004, vol. 40, no. 2, pp. 410−417.

12. Korovkin, N.V., Chechurin, V.L., and Hayakawa, M., *Inverse Problems in Electric Circuits and Electromagnetics*, New York: Springer, 2007.

13. Galchenko, V.Ya., Yakimov, A.N., and Ostapushchenko, D.L., Solution of the inverse problem of creating a uniform magnetic field in coercimeters with partially closed magnetic systems, *Rus. J. Nondestr. Test.*, 2011, vol. 47, no. 5, pp. 295−307.

14. Halchenko, V.Ya., Ostapushchenko, D.L., and Vorobyov, M.A., Mathematical simulation of magnetization processes of arbitrarily shaped ferromagnetic test objects in fields of given spatial configurations, *Rus. J. Nondestr. Test.,* 2008, vol. 44, no. 9, pp. 589−600.

15. Galchenko, V.Ya., Ostapushchenko, D.L., and Vorobyov, M.A., Computer analysis of the configuration of the magnetic fields of surface discontinuity flaws of finite dimensions in a ferromagnetic plate of finite dimensions by the spatial integral equation method, *Rus. J. Nondestr. Test.*, 2009, vol. 45, no. 3, pp. 191−198.

16. Galchenko, V.Ya., Ostapushchenko, D.L., and Vorobyov, M.A., Computer analysis of the configurations of magnetic fields of subsurface discontinuities of finite dimensions and arbitrary shapes in test objects of finite length by the method of spatial integral equations*, Rus. J. Nondestr. Test.*, 2009, vol. 45, no. 5, pp. 337−346.

17. Gal'chenko, V.Ya., Ostapushchenko, D.L., and Vorob'ev, M.A., Numerical simulation of the circular and pole magnetization of straight-seam electric-welded pipes during their magnetic nondestructive testing, *Kontrol'. Diagnostika,* 2009, no. 11, pp. 18−27.

18. Gal'chenko, V.Ya. and Vorob'ev, M.A., Structural synthesis of attachable eddy-current probes with a given distribution of the probing field in the test zone, *Rus. J. Nondestr. Test.*, 2005, vol. 41, no. 1, pp. 29−33.

19. Li, M. and Lowther, D.A., The application of topological gradients to defect identification in magnetic flux leakage-type NDT, *IEEE Trans. Magn.,* 2010, vol. 46, no. 8, pp. 3221−3224.

20. Gal'chenko, V.Ya. and Ostapushchenko, D.L., Numerical analysis of the spatial configuration of magnetic fields from objects with complex shapes with allowance for nonlinear material characteristics, *Inform. Tekhnol.*, 2008, no. 8, pp. 43–49.

21. Gal'chenko, V.Ya., Yakimov, A.N., and Ostapushchenko, D.L., Multi-criteria synthesis of axially symmetric magnetic systems with ferromagnetic elements and a specified magnetic field configuration, *Elektrichestvo*, 2012, no. 4, pp. 40–54.

22. Gal'chenko, V.Ya., Yakimov, A.N., and Ostapushchenko, D.L., Pareto-optimal parametric synthesis of axisymmetric magnetic systems with allowance for nonlinear properties of the ferromagnet, *Tech. Phys.*, 2012, vol. 57, no. 7, pp. 893–899.

23. Gal'chenko, V.Ya., Yakimov, A.N., and Ostapushchenko, D.L., Search for a global optimum of functions using the hybrid of multi-agent swarm optimization with the evolutionary formation of a population composition, *Inform. Tekhnol.*, 2010, no. 10, pp. 9–16.

24. Hopcroft, J.E., Motwani, R., and Ullman, J.D., *Introduction to Automata Theory, Languages, and Computation,* Boston: Addison-Wesley, 2000.

25. Rastrigin, L.A., *Adaptatsiya slozhnykh system: metody i prilozheniya* (Adaptation of Complex Systems: Methods and Applications), Riga: Zinatne, 1981.

Translated by E. Glushachenkova